Chemical Engineering Journal 149 (2009) 123–131

Contents lists available at ScienceDirect

Chemical Engineering Journal

journal homepage: www.elsevier.com/locate/cej

Characterization and properties of iron oxide-coated zeolite as adsorbent for removal of copper(II) from solution in fixed bed column

Runping Han[a,b,*], Lina Zou[a], Xin Zhao[c], Yanfang Xu[a], Feng Xu[a], Yinli Li[a], Yu Wang[a]

[a] Department of Chemistry, Zhengzhou University, No 75 of Da Xue North Road, Zhengzhou, 450052 PR China
[b] China Petroleum & Chemical Cooperation Luoyang Company, Jili District, Luoyang, 471012 PR China
[c] School of Chemistry and Chemical Engineering, Sun Yat-Sen University, No 135 of Xingang West Road, Guangzhou, 510275 PR China

ARTICLE INFO

Article history:
Received 21 July 2008
Received in revised form
28 September 2008
Accepted 6 October 2008

Keywords:
Iron oxide-coated zeolite (IOCZ)
Copper ion
Column adsorption
Dynamic model

ABSTRACT

A new composite adsorbent, iron oxide coated zeolite (IOCZ), was characterized and employed for the removal of Cu(II) from aqueous solution using fixed bed column. Scanning electron microscope (SEM), FTIR, X-ray diffraction spectrum (XRD) and BET analyses were used to study the surface properties of the coated layer. The effects of various experimental conditions, such as the flow rate, initial metal concentration and bed depth, were studied. The dynamics of the adsorption process were fitted by Adams–Bohart model and Thomas model. The Thomas model was found suitable for the description of breakthrough curve at all experimental conditions, while Adams–Bohart model was only for an initial part of dynamic behavior of the IOCZ column. The bed depth service time (BDST) model was applied to predict the service times with other flow rate and initial concentration. The theoretical breakthrough curve was compared with experimental breakthrough curve profile in the dynamic process. The saturated column was regenerated by 1 mol l^{-1} hydrogen chloride solution and IOCZ could be reused in Cu(II) removal.

1. Introduction

It is well known that copper is a very common metal, which is widely used in electroplate, light industry, mechanical manufacturing industry and architecture. Additionally, copper is an indispensable micronutrient to humans and other life forms. However, it is one of the toxic metals to human beings as excessive copper would cause serious lesions in the central nervous system and even permanent damage particularly for children [1]. With the increasing discharge of industrial wastewater, copper has been listed as one of the most widespread heavy metal contaminants [2]. Thus, it is quite necessary to remove heavy metals from wastewater.

Up to now, various traditional treatment technologies including chemical precipitation, filtration, ion exchange and activated carbon adsorption on a solid heterogeneous surface are widely applied and have been developed [3–7]. These methods, however, display one or more limitations, such as ineffective, expensive, generation of secondary pollution and narrow appliance range. Overcoming these limitations, chemists have been devoted to search for effective, economic and easily implemented materials [8–12].

Natural zeolite, as aluminosilicate mineral, has characteristics of large surface area, strong capability of ions exchange and adsorption for their particular tetrahedral pore framework. Moreover, they are one of low-cost and easily obtaining materials which have been used as an adsorption for removal of heavy metals [12–18]. In order to enhance the sorption capacity of natural zeolite for heavy metal ions, some researchers modified their surface by metal oxide. Because iron, manganese, aluminum oxides have a large area and high affinity toward metal ions, these metal oxide-coated materials have been investigated, and these composites have effective absorbability for heavy metal removal from wastewater [19–24].

There are seldom papers about the study of a new composite, iron oxide-coated zeolite (IOCZ) as adsorbent for removal metals and other pollutant from water. This study was designed to test the fixed bed column performance of IOCZ as an adsorbent for the removal of copper ion from synthetic solution in a continuous flow system. The property of IOCZ surface was first analyzed. Then the effects of flow rate, influent concentration and bed height on copper adsorption by IOCZ were investigated, respectively. The dynamic process of adsorption was modeled by Adams–Bohart model, Thomas model, BDST model and mass transfer model. Finally, regeneration of the IOCZ bed saturated with copper ions

* Corresponding author at: Department of Chemistry, Zhengzhou University, No 75 of Da Xue North Road, Zhengzhou, 450052 PR China. Tel.: +86 371 67781757; fax: +86 371 67781556.
E-mail address: rphan67@zzu.edu.cn (R. Han).

1385-8947/$ – see front matter © 2008 Elsevier B.V. All rights reserved.
doi:10.1016/j.cej.2008.10.015

was also conducted using 1 mol l^{-1} HCl to assess whether IOCZ was able to efficiently regenerate and reuse.

2. Materials and methods

2.1. Preparation of IOCZ

The raw zeolite used in the study was obtained from Xinyang city in China. The raw zeolite was sieved to get average size particles about 20–40 mesh. Before used, they were immersed in distilled water for 24 h, and changed the water every 4 h, then roasted them at 300 °C in muffle furnace for 1 h, prepared for surface coating.

Mixed 50 g pretreated zeolite and 50 ml ferric chloride solution of 1 mol l^{-1}, and stirred to make them contacted sufficiently. The mixture was kept at 80 °C using water bath and 50 ml sodium hydroxide solution of 3 mol l^{-1} was slowly poured into the mixture with slight stirring. Then placed mixture in muffle furnace and keeping at 500 °C for 4 h after reaction. Next, the mixture was cooled to room temperature and washed to pH 7.0 using distilled water. Finally, the sample was dried at 110 °C, and stored in polypropylene bottle for use.

The removal capacity of IOCZ was compared with that of raw zeolite. In batch experiments (temperature 273 K, adsorbent dose 0.04 g, 10 ml 30 mg l^{-1} Cu^{2+} solution), the equilibrium adsorption capacities for zeolite and IOCZ were found to be 3.88 mg g^{-1} zeolite and 5.14 mg g^{-1} IOCZ for Cu(II), respectively. The results indicated that the adsorption capacity of IOCZ is bigger than that of raw zeolite for the removal of Cu(II).

2.2. Characterization of IOCZ

Photomicrography of the exterior surface of uncoated zeolite and IOCZ was obtained by SEM (JEOL6335F-SEM, Japan). Samples for an energy dispersive analysis of X-ray (EDAX) were coated with a thin carbon film in order to avoid the influence of any charge effect during the SEM operation.

Analyses of the physical characteristics of IOCZ included specific surface area and pore size distributions. The specific surface area of IOCZ and pore volumes were tested using the nitrogen adsorption method with a NOVA 1000 high speed, automated surface area and pore size analyzer (Quantachrome Corporation, U.S.), and the BET adsorption model was used in the calculation. Calculation of pore size followed the method according to implemented software routines.

The mineralogy of the sample was characterized by X-ray diffraction (XRD) (Tokyo Shibaura Model ADG-01E). The FTIR of raw zeolite and IOCZ was also presented using FTIR instrument (PE-1710 FTIR).

2.3. Metal solution

All chemicals used for the study were analytical grades of copper chloride ($CuCl_2$) and hydrochloride acid supplied by Luoyang Chemical reagent company (China). The stock solution (1000 mg l^{-1}) of copper was prepared by dissolving the salts in distilled water. The initial pH of the working solution was adjusted to 4 by addition of HNO_3 or NaOH solution. No other solutions to provide additional ionic strength.

2.4. Methods of adsorption studies

Column experiments were operated with 0.95 cm diameter glass column at 273 K to evaluate the effects of initial Cu(II) concentration, the flow rate, and the bed depth. The bed depths taken were 6 cm (3 g), 11 cm (5.5 g) and 15 cm (8 g). For different bed depths, the initial Cu(II) concentration of the solution was 60 mg l^{-1}. The column performance of Cu adsorption onto IOCZ was also studied at Cu concentration of 40 mg l^{-1} and 80 mg l^{-1}, keeping bed depth 11 cm and flow rate 11 ml min^{-1}. In addition, the effect of different flow rates, 8 ml min^{-1} and 14 ml min^{-1}, were investigated at the same Cu(II) concentration (60 mg l^{-1}) and bed depth (11 cm), respectively. The metal solution was pumped to the column in a down-flow direction by a peristaltic pump at a certain rate. Samples were collected at regular intervals and in all the adsorption and desorption experiments, the concentration of Cu(II) ions in the effluent was analyzed using flam atomic absorption spectrometer (AAS) (AAanalyst300, PerkinElmer). The detection limit of copper ions was 0.05 mg l^{-1}. The concentration of copper ions desorbed from ICOZ column by 1 mol l^{-1} hydrogen chloride solution was also analyzed.

2.5. Column model

The loading behavior of Cu(II) to be removed from solution in a fixed bed was usually expressed in term of C_t/C_0 (C_t = effluent metal ions concentration and C_0 = influent metal ions concentration) as a function of time or volume of the effluent for a given bed height, thus the breakthrough curves were obtained [24].The maximum column capacity, q_{total} (mg), for a given feed concentration and flow rate is equal to the area under the plot of the adsorbed Cu(II) concentration C_{ad} ($C_{ad} = C_0 - C$) (mg l^{-1}) versus effluent time (t, min) and is calculated from Eq. (1):

$$q_{total} = \frac{QA}{1000} = \frac{Q}{1000}\int_{t=0}^{t=t_{total}} C_{ad}\,dt \quad (1)$$

where t_{total}, Q and A are the total flow time (min), volumetric flow rate (ml min^{-1}) and the area under the breakthrough curve, respectively.

The equilibrium uptake ($q_{eq(exp)}$), the weight of Cu(II) adsorbed per unit dry weight of adsorbent (mg g^{-1}) in the column, is calculated as following:

$$q_{eq(exp)} = \frac{q_{total}}{m} \quad (2)$$

where m is the total dry weight of IOCZ in column (g).

Total amount of Cu(II) sent to column(W_{total}) is calculated from Eq. (3)

$$W_{total} = \frac{C_0 Q t_{total}}{1000} \quad (3)$$

Total removal percent of Cu(II) is the ratio of the maximum capacity of the column (q_{total}) to the total amount of Cu(II) sent to column(W_{total}).

$$Y = \left(\frac{q_{total}}{W_{total}}\right) \times 100 \quad (4)$$

For the successful design of a column adsorption process, it is important to predict the breakthrough curve for the effluent. Various kinetics models have been developed to predict the dynamic behavior of the column.

2.5.1. The Adams–Bohart model

The Adams–Bohart model is used for the description of the initial part of the breakthrough curve. The expression is the following [25]:

$$\frac{C_t}{C_0} = \exp\left(k_{AB}C_0 t - k_{AB}N_0\frac{Z}{F}\right) \quad (5)$$

where k_{AB} is the kinetic constant (l mg^{-1} min^{-1}), F is the linear flow rate (cm min^{-1}), Z is the bed depth of column (cm) and N_0

is the saturation concentration (mg l^{-1}). The value of t is time (min, $t = V_{eff}/\nu$), V_{eff} is the volume of effluent solution (ml), ν the flow rate (ml min^{-1}).

Values describing the characteristic operational parameters (k_{AB} and N_0) of the column can be calculated using nonlinear regression analysis according to Eq. (5).

2.5.2. Thomas model

The expression of Thomas model for an adsorption column is given as follows [26]:

$$\frac{C_t}{C_0} = \frac{1}{1 + \exp(k_{Th}q_0 m/\nu - k_{Th}C_0 t)} \tag{6}$$

where q_0 the equilibrium Cu(II) uptake per g of the adsorbent (mg g^{-1}).

The values of k_{Th} and q_0 can be determined from a plot of C_t/C_0 against t using nonlinear regression analysis as the values of C_t/C_0 is within 0.05–0.95.

2.5.3. The bed-depth/service time analysis (BDST) model

The BDST model describes a relation between the service time and the packed-bed depth of the column and is expressed as [27]:

$$t = \frac{N_0}{C_0 F}Z - \frac{1}{K_a C_0}\ln\left(\frac{C_0}{C_t} - 1\right) \tag{7}$$

where K_a is the rate constant in BDST model (l mg^{-1} min^{-1}).

A plot of t versus bed depth, Z, should yield a straight line where N_0 and K, the adsorption capacity and rate constant, can be evaluated respectively.

A simplified form of the BDST model is:

$$t = aZ - b \tag{8}$$

where

$$a = \frac{N_0}{C_0 F} \tag{9}$$

$$b = \frac{1}{K_a C_0}\ln\left(\frac{C_0}{C_t} - 1\right) \tag{10}$$

The slope constant for a different flow rate can be directly calculated by Eq. (11):

$$a' = a\frac{F}{F'} = a\frac{\nu}{\nu'} \tag{11}$$

where a and F are the old slope and influent linear velocity, respectively, and a' and F' are the new slope and influent linear velocity. As the column used in experiment has the same diameter, the ratio of original (F) to the new influent linear velocity (F') and original flow rate (ν) to the new flow rate (ν') is equal. For other influent concentrations, the desired equation is given by a new slope, and a new intercept given by:

$$a' = a\frac{C_0}{C_0'} \tag{12}$$

$$b' = b\frac{C_0}{C_0'}\frac{\ln(C_0' - 1)}{\ln(C_0 - 1)} \tag{13}$$

where b', b are the new and old intercept, respectively, C_0' and C_0 are the new and old influent concentration, respectively.

2.5.4. Error analysis

In order to evaluate the fitness of Adams–Bohart model and Thomas models to the experimental dynamic data, an error function is required to enable the optimization procedure, combining the values of determined coefficient (R^2) from regressive analysis. In this study, the values of SS were examined.

$$SS = \sqrt{\sum \frac{(y_e - y_c)^2}{n}} \tag{14}$$

where n is the number of experimental data points, y_c is the predicted (calculated) data and y_e is the experimental data [28,29].

2.5.5. The mass transfer model

The data obtained from the batch adsorption isotherm can be used to predict the theoretical breakthrough curve, which can be well compared with the experimental curve. The detailed calculations for the generation of the experimental breakthrough curve from the equilibrium data obtained from batch studies are as follows [14,30]:

(1) An experimental equilibrium curve is drawn assuming various values of C_e (the value is equal to C_t) and calculating the corresponding values of q_e using the best fit isotherm model obtained from the batch results.
(2) An operating line is drawn, which was passing through the original and end points obtained by experimental equilibrium curve. The significance of this operating line is that the data of the continuously batch reactor and the data of the fixed bed reactor are identical at these two points, first at the initiation and other at the exhaustion of the reaction.
(3) According to Weber, the rate of transfer of solute from solution over a differential depth of column, dh, is given by Eq. (15):

$$\nu dC = K_a'(C - C*)dh \tag{15}$$

where ν is the wastewater flow rate, K_a' the overall mass transfer coefficient, which includes the resistances offered by film diffusion and pore diffusion and C^* is the equilibrium concentration of solute in solution corresponding to an adsorbed concentration, q_e.

The term $(C - C^*)$ is the driving force for adsorption and is equal to the distance between the operating line and equilibrium curve at any given value of q_e. Integrating Eq. (15) and solving for the height of the adsorption zone:

$$h_z = \frac{\nu}{K_a'}\int_{C_B}^{C_E}\frac{dC}{C - C^*} \tag{16}$$

For any value of h less than h_z, corresponding to a concentration C between C_B and C_E, Eq. (16) can be written as:

$$h = \frac{\nu}{K_a'}\int_{C_B}^{C}\frac{dC}{C - C^*} \tag{17}$$

Dividing Eq. (17) by Eq. (16) results in Eq. (18)

$$\frac{h}{h_Z} = \frac{\int_{C_B}^{C} dC/(C - C*)}{\int_{C_B}^{C_E} dC/(C - C*)} = \frac{V - V_B}{V_E - V_B} \tag{18}$$

where V_B and V_E are total volume of water treated till breakthrough and up to exhaust point, respectively, and V is the volume of water treated within V_E for effluent concentration C within C_E. Dividing the values of $\int_{C_B}^{C} dC/(C - C*)$ by the value of $\int_{C_B}^{C_E} dC/(C - C*)$ the term $(V–V_B)/(V_E–V_B)$ was evaluated.
(4) Now the plot of C_t/C_0 versus $(V–V_B)/(V_E–V_B)$ represents the theoretical breakthrough curve.

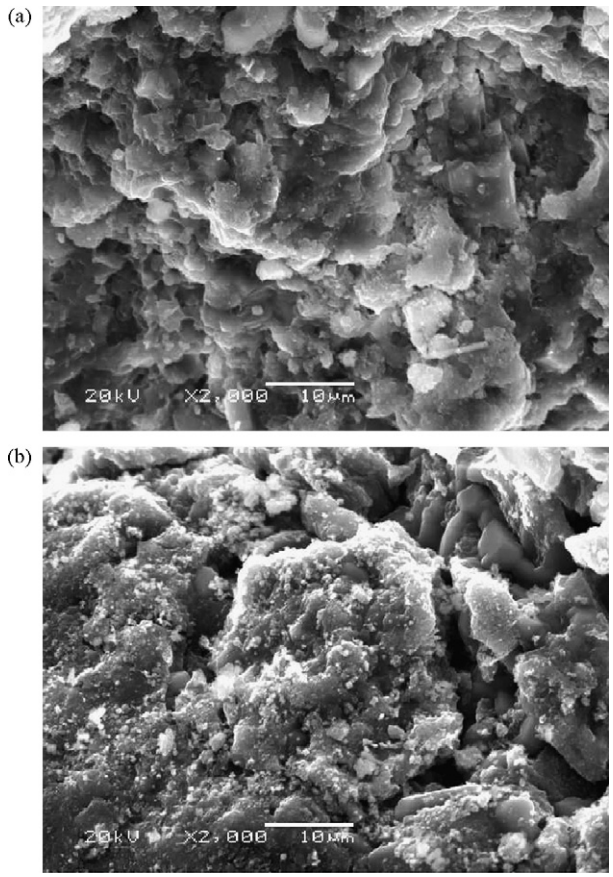

Fig. 1. SEM micrograph of samples: (a) zeolite and (b) IOCZ.

3. Results and discussion

3.1. Characterization

3.1.1. Mineralogy of IOCZ and results of EDAX

The samples of zeolite coated with iron oxide were dark red colored precipitates, indicating the presence of iron in the form of insoluble oxides. The SEM photographs in Fig. 1 were taken at 2000 magnification to observe the surface morphology of zeolite and IOCZ, respectively. The surface coverage of zeolite by iron oxides was observed by comparing the images of virgin (Fig. 1a) and IOCZ (Fig. 1b). The coated zeolite surfaces were apparently occupied by newborn iron oxides, which were formed during the coating process. Fig. 1b also showed iron oxides, formed in clusters, apparently on occupied surfaces. At the micron scale, the synthetic coating was composed of small particles on top of a more consolidated coating.

In conjunction with electron microscopy, elemental identifications of surface features were performed by qualitative EDAX analysis. The EDAX results are following: There are O (48.10%), Mg (0.52%), Al (6.21%), Si (40.21%), K (3.29%), Ca (0.20%), Fe (1.47%) in surface of zeolite by EDAX analysis, while O (22.56%), Cl (9.45%), Na (3.95%), Si (5.47%), K (3.29%), Ca (1.40%), Fe (47.17%) in surface of IOCZ. EDAX analysis yielded direct evidence for iron oxide coated on the surface of zeolite.

3.1.2. XRD of zeolite and IOCZ

The XRD Spectra of zeolite (a) and IOCZ (b) were shown in Fig. 2.

From Fig. 2, the mineralogical composition of zeolite was comprised primarily of clinoptilolite (2θ: 22°, 23°, 28°) and additionally of feldspar, montmorillonite and quartz by means of XRD [31]. Compared to XRD of zeolite, XRD of ICOZ contained the peak of iron oxide (2θ: 27°), other peaks were from the zeolite.

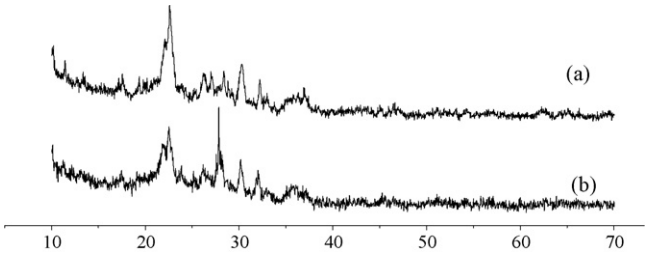

Fig. 2. The XRD of zeolite (a) and ICOZ (b).

3.1.3. Specific surface area and pore size distribution analyses

The surface area of IOCZ increased from 24.87 to 29.35 $m^2\ g^{-1}$ after coating iron oxide on the surface of zeolite, while the average pore diameter decreased from 28.66 to 27.12 Å.

3.1.4. FTIR of zeolite and IOCZ

Fig. 3 showed the FTIR of zeolite and IOCZ. From Fig. 3, the FTIR spectra of zeolite composed of the peaks of sorbed water, vibration of framework and Si–O or Al–O [31,32]. Compared to FTIR of zeolite, FTIR of ICOZ was similar to zeolite, this was due to the small content of iron in ICOZ and the sample of FTIR was treated as powder. So the peaks of iron oxide were masked by those from zeolite.

3.2. Influence of operating conditions on column sorption of Cu ion

Operational conditions, such as flow rate, initial feed concentration and bed depth, are important for column design. We studied the effects of these parameters on the adsorptive behavior capacity of IOCZ for Cu(II) adsorption.

3.2.1. Effect of flow rate and initial concentration on breakthrough

The breakthrough curves at various flow rates and initial concentration of metal ion were shown in Figs. 4 and 5.

From the Figs. 4 and 5, it was shown that adsorption arrived saturation faster with increasing flow rate and influent Cu(II) concentration. The exhaust times (corresponding to 90% of influent concentration) for flow rates 8, 11 and 14 ml min^{-1} were found to be 680, 300 and 210 min, respectively. For influent Cu(II) concentration 40, 60 and 80 mg l^{-1}, the exhaust times were 521, 300 and 160 min, respectively. This tendency was consistent to other researches [14,26–28]. When at higher flow rate, the external film mass resistance at the surface of the adsorbent tends to decrease and the residence time of the effluent inside the column decreases, hence the time required to reach saturation decreases, and in turn gives the lower removal efficiency [33,34]. Higher initial influent concentrations lead to higher mass transfer driving force, hence Cu(II) concentrations saturate the adsorbent more quickly, which results in a decrease of exhaust time. As influent concentration increases, sharper breakthrough curves can be obtained.

3.2.2. Effect of bed depth on breakthrough

The breakthrough curves at various bed depths were shown in Fig. 6.

The experimental exhaust times reaching saturation for bed depths 6, 11 and 15 cm were found to be 135, 300 and 460 min, respectively. It was clearly that as the bed depth increased, the exhaust time increased due to the increased binding sites of the

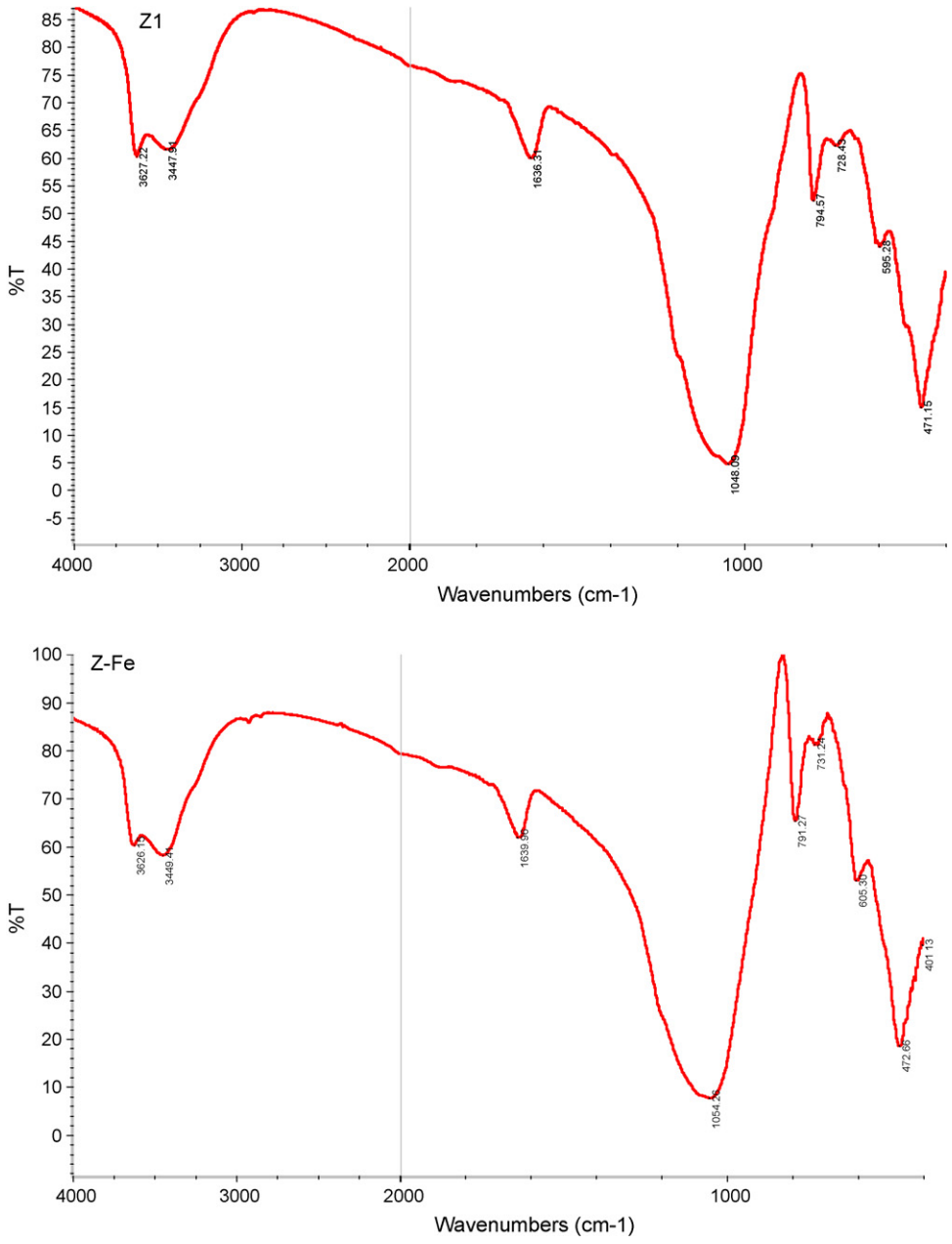

Fig. 3. FTIR of zeolite and IOCZ.

column. On the other hand, more contact time of adsorbent/Cu(II) resulted in higher removal efficiency.

3.3. Evaluation of breakthrough curves

3.3.1. The Adams–Bohart model

The Adams–Bohart adsorption model was applied to describe the initial part of the breakthrough curve (the concentration $C_t < 0.5C_0$). This approach was focused on breakthrough, for all breakthrough curves using nonlinear regression analysis, relative values of N_0, and k_{AB} were calculated and presented in Table 1. As seen from Table 1, the value of N_0 increased with the increasing bed depth and decreasing flow rate, while the value of k_{AB} decreased. Table 1 also presented the value of R^2 obtained from nonlinear analysis ($R^2 > 0.869$) and SS (less than 0.061). The breakthrough curves predicted from the Adams–Bohart model were compared with the experimental points and were also shown in Figs. 1–3, respectively. It was clear from Figs. 1–3 and Table 1 that there was a good agreement between the experimental points and predicted values, suggesting that Adams–Bohart model may be valid for the adsorption processes where relative concentration region was up to 0.5 at all operating conditions.

Although the Adams–Bohart model provides a simple and comprehensive approach to evaluate sorption column test, its validity is limited in the range of conditions used [14].

3.3.2. Thomas model

The Thomas model was fitted to investigate the breakthrough behavior of Cu(II) onto IOCZ. The Thomas rate constant (k_{Th}) and maximum solid-phase concentration (q_0) were obtained using nonlinear regression analysis according Eq. (6) and the results were listed in Table 2. The values of SS (less than 0.094) and $q_{eq(exp)}$ at

Table 1
Adams–Bohart parameters at different conditions using nonlinear regression analysis (up 50%).

C_0 (mg l^{-1})	v (ml min^{-1})	Z (cm)	$K_{AB} \times 10^3$ (l mg^{-1} min^{-1})	N_0 (mg l^{-1})	R^2	SS
60	11	6	0.998 ± 0.022	3172 ± 0.84	0.903	0.048
60	11	11	0.573 ± 0.078	7319 ± 0.78	0.969	0.0304
60	11	15	0.425 ± 0.094	9378 ± 1.2	0.923	0.0483
60	8	11	0.33 ± 0.089	8018 ± 2.2	0.869	0.0609
60	14	11	1.02 ± 0.2045	5173 ± 0.63	0.915	0.0522
40	11	11	0.549 ± 0.16	8100 ± 2.9	0.903	0.0524
80	11	11	0.552 ± 0.3	7049 ± 0.90	0.935	0.0393

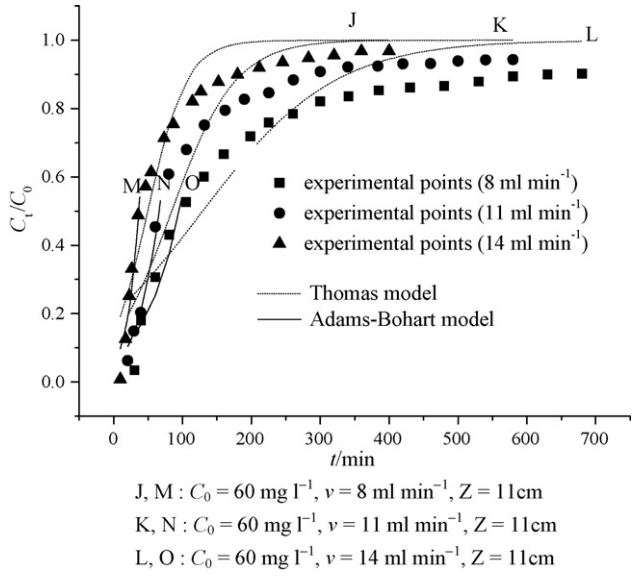

Fig. 4. Experimental and predicted breakthrough curves of Cu(II) adsorption onto IOCZ at different flow rates.

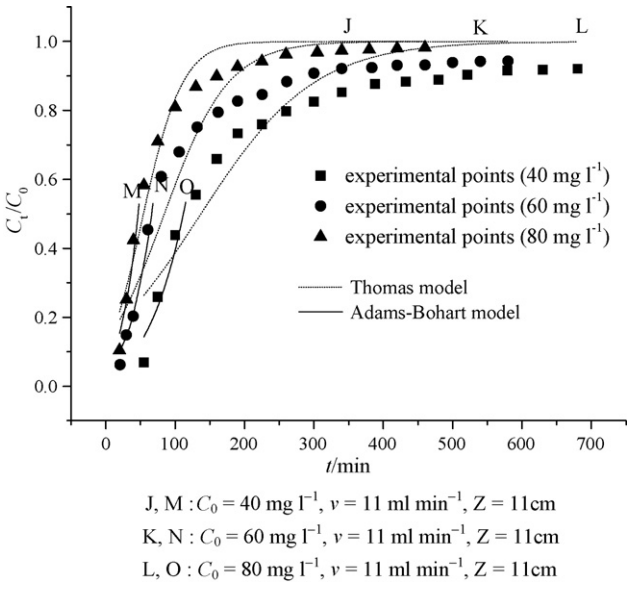

Fig. 5. Experimental and predicted breakthrough curves of Cu(II) adsorption onto IOCZ at different initial concentrations.

various conditions were also listed in Table 2. Analysis of the regression coefficients indicated that the regressed lines provided good fit to the experimental data with R^2 values ranging from 0.87 to 0.96, which were higher as there were more than 21 experimental points. As shown in Table 2, with the flow rate and initial concentration increasing, the values of k_{Th} became bigger, while the q_0 became smaller. With the bed depth increasing, the value of q_0 changed slightly. The trend of $q_{eq(exp)}$ change is familiar with q_0. Furthermore, the value of q_0 obtained from experiment was different from calculated result at the same condition. Compared with other adsorbents, the adsorption capacity of IOCZ was relatively lower, however the efficiency can be achieved for their low cost [17,24,35]. Figs. 1–3 also showed the comparison of the experimental points and predicted curves using Thomas model at various operating conditions. The results in the figures clearly indicated that predicted curves proposed by Thomas model were in good agreement with the experimental curves at all experimental conditions.

Table 3
Calculated constants of BDST model for the adsorption of Cu (C_0 = 60 mg l^{-1}, v = 11 ml min^{-1}).

C_t/C_0	a (min cm^{-1})	b (min)	K_a (l mg^{-1} min^{-1})	N_0 (mg l^{-1})	R^2	SS
0.2	3.84	9.40	0.00242	2536	0.989	10.5
0.4	5.66	11.3	0.000534	3736	0.995	8.66
0.6	8.57	14.1	0.00052	5653	0.999	1.61

3.3.3. BDST model

The BDST model was used to evaluate the feasibility of the design of adsorption column for changed flow rate and initial concentration. According to Eqs. (7) and (8), the value of related parameters of BDST and SS at C_t/C_0 0.2, 0.4 and 0.6 were shown in Table 3. With the increased C_t/C_0, the values of N_0 increased while K_a decreased. The values of R^2 and SS indicated the validity of BDST model for present system.

The BDST equation obtained at flow rate 14 ml min^{-1} and influent concentration 80 mg l^{-1} was used to predict the adsorbent

Table 2
Thomas parameters at different conditions using nonlinear regression analysis.

C_0 (mg l^{-1})	v (ml min^{-1})	Z (cm)	$q_{eq(exp)}$ (mg g^{-1})	$q_{0(cal)}$ (mg g^{-1})	K_{Th} (ml min^{-1} mg^{-1})	R^2	SS
60	11	6	12.4	7.54 ± 0.0016	0.721 ± 0.092	0.948	0.0637
60	11	11	14.7	11.1 ± 0.0026	0.370 ± 0.058	0.917	0.0817
60	11	15	13.5	8.94 ± 0.0027	0.242 ± 0.41	0.871	0.0910
60	8	11	16.2	11.3 ± 0.0047	0.177 ± 0.029	0.866	0.0935
60	14	11	11.3	7.57 ± 0.0014	0.603 ± 0.095	0.924	0.0824
40	11	11	15.0	10.9 ± 0.0051	0.311 ± 0.053	0.878	0.0855
80	11	11	11.9	8.68 ± 0.0014	0.471 ± 0.063	0.959	0.0555

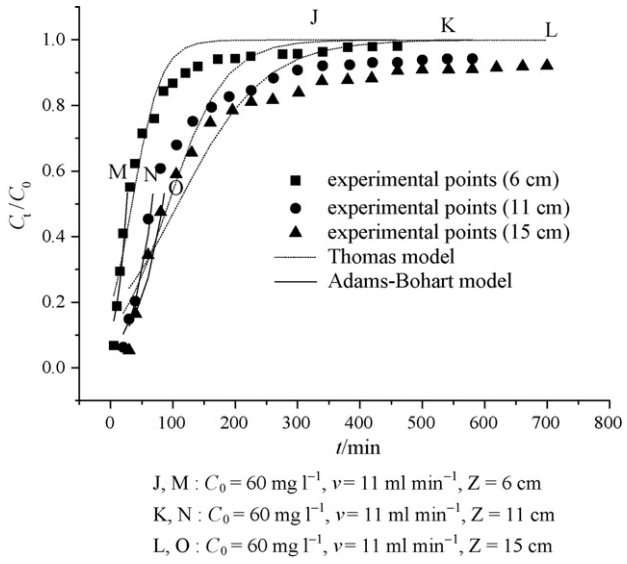

Fig. 6. Experimental and predicted breakthrough curves of Cu(II) adsorption onto IOCZ at different bed depths.

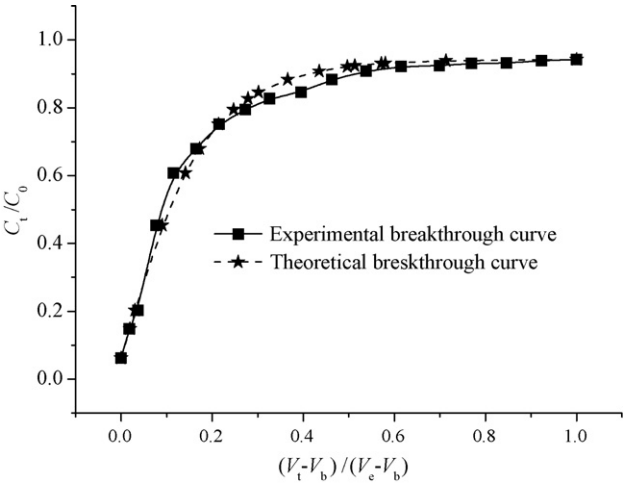

Fig. 7. Measured and predicted breakthrough curve according to the mass transfer model (C_0 = 60 mg l^{-1}).

performance at lower flow rates of 11 ml min^{-1} and influent concentration of 60 mg l^{-1}, respectively. The predicted time (t_c) and experimental time (t_e) were shown in Table 4. From Table 4, the calculated time and experimental values were well consistent with each other, indicating that the BDST model can be used to predict adsorption performance at other operating conditions for adsorption of Cu(II) onto IOCZ in fixed bed column.

3.3.4. Mass transfer model based on batch isotherm studies to the experimental data

According to mass transfer model, the date obtained from the batch isotherm studies can be used to predict the theoretical breakthrough curve, which can be compared with the experimental breakthrough curve. Evaluating the result from fitting the batch experimental data to the Langmuir, Freundlich, Temkin, Redlich–Peterson and Koble–Corrigan isotherm [36], it was showed that Redlich–Peterson isotherm (R^2 = 0.999) provided a best fitness compared to others (Langmuir 0.990, Freundlich 0.918, Temkin 0.956, Koble–Corrigan 0.985). So the Redlich–Peterson isotherm ($q_e = AC_e/(1 + BC_e^g)s$) was used to generate the theoretical breakthrough curve. Fig. 7 showed the theoretical breakthrough curve compared with the experimental breakthrough curve which relevant to 11 cm bed depth and initial Cu(II) concentration of 60 mg l^{-1}. The two curves followed the same trend with small differences. Therefore, Redlich–Peterson isotherm constants found from the batch experimental data can be used to predict the breakthrough in fixed bed system for Cu(II) adsorption onto IOCZ.

Table 4
Predicted breakthrough time based on the BDST constants for a new flow rate (v = 14 ml min^{-1}, Z = 6 cm) and a new influent concentration (Z = 6 cm, C_0 = 80 mg l^{-1}).

C_t/C_0	Z (cm)	v' (ml min^{-1})	t_c (min)	t_e (min)	C_0' (mg l^{-1})	t_c (min)	t_e (min)
0.2	6	14	23.8	20.8	80	24.1	26.6
0.4	6	14	37.6	31.1	80	37.6	39.2
0.6	6	14	59.9	53.4	80	59.3	58.7

3.4. Desorption of Cu(II) and regeneration of IOCZ

Disposal of the exhausted adsorbent loaded with heavy metal ions can create another environmental problem as it is hazardous material which pollutes environment. This problem may be overcome to some extent by using one of the elimination (e.g. elution, incineration and pyrolysis) methods. The elution of heavy metals is the most common elimination method, allowing both recovery of solutions of heavy metal ions at higher concentrations for inertisation and recycling of the adsorbent for subsequent uses. Regeneration of the adsorbent material is of crucial importance in the economic development [37].

Once the column reached exhaustion, it is important to regenerate IOCZ for the recovery of metal ions as well as the reuse of IOCZ for adsorption. Fixed bed column regeneration study was conducted to assess the possibilities for the reuse of the adsorbent and recovery of metal ions. Firstly, 6 cm depth of IOCZ was saturated by influent solution of 60 mg l^{-1} initial Cu(II) concentration at the flow rate of 11 ml min^{-1}. Then the exhausted IOCZ was regenerated using 1 mol l^{-1} HCl solution at the same flow rate. Next, the column was washed with distilled water until the pH of effluent water reached 4.0. In this paper, we repeated the above process three times. Figs. 8 and 9 showed three consecutive desorption and sorption cycles (C_t in Y axis is the Cu^{2+} concentration of elution

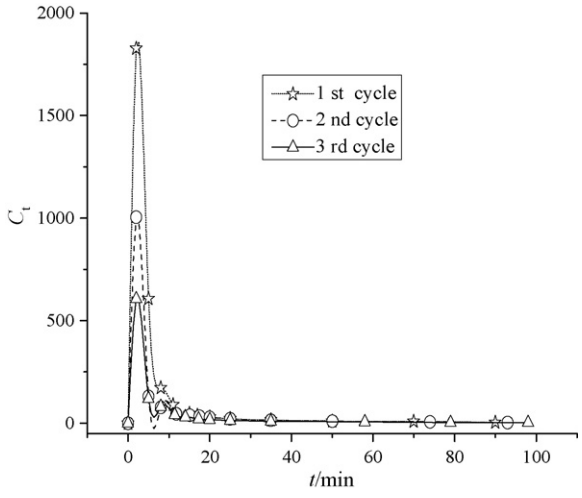

Fig. 8. Desorption of Cu(II) for three cycles.

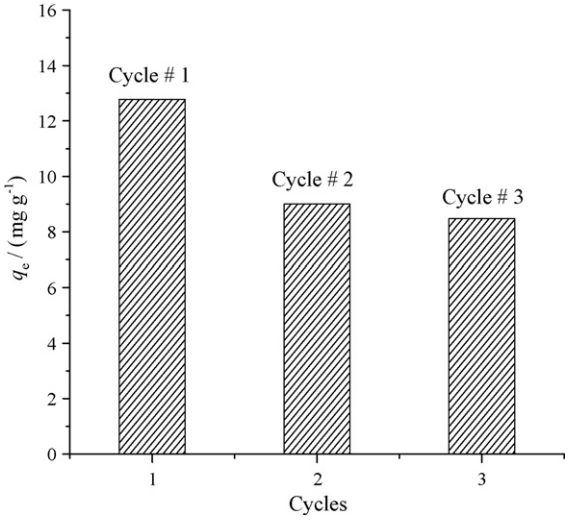

Fig. 9. Cu(II) removal capacity of IOCZ during three consecutive cycles (C_0 = 60 mg l^{-1}, v = 11 ml min^{-1}, Z = 6 cm).

solution). The figures indicated that Cu(II) was easily desorbed because the desorption completed in less than 20 min, before 5 min, the effluent Cu(II) concentration was very high which was beneficial to metal recovery. Fig. 9 indicated that the removal capacity of IOCZ decreased at a certain extent in the second cycle, but there was no obvious change in the third cycle which decreased by not more than 6%. Hence, it was proved that the regeneration and reuse of IOCZ was an economical and efficient method for removal of Cu(II) from water. From the results of desorption and regeneration using HCl solution, ion exchange was an important mechanism of Cu(II) adsorption onto ICOZ [24,37].

4. Conclusion

In this study, ICOZ was characterized. Experimental and theoretical investigations were carried out to evaluate the fixed bed column performance of Cu(II) removal from aqueous solution onto IOCZ. The following conclusion was drawn:

(1) Iron oxide coated in the surface of zeolite was characterized by SEM, EDAX and XRD analysis.
(2) This study showed that IOCZ was an effective adsorbent for removal of Cu(II) from aqueous solution.
(3) The adsorption of Cu(II) was strongly dependent on the flow rate, the initial Cu(II) concentration and bed depth.
(4) At all experimental condition, the whole breakthrough process can be described by Thomas while the initial region of breakthrough curve was defined by Adams–Bohart model.
(5) The breakthrough data predictions by BDST model showed good agreement with experiment data.
(6) The mass transfer model could provide a good agreement between the experimental breakthrough curve and theoretical breakthrough curve.
(7) Copper ions were easily desorbed from the IOCZ column using 1 mol l^{-1} HCl solution and the ICOZ column can be reused to remove Cu(II) from aqueous efficiently.

Acknowledgment

The authors express their sincere gratitude to the Education Department of Henan Province in China for the financial support of this study.

References

[1] G. McKay, Y.S. Ho, J.C.P. Ng, Biosorption of copper from waste waters: a review, Sep. Purif. Methods 28 (1999) 87–125.
[2] S.G. Dai, Environmental Chemistry, Higher Education Press, Beijing, 1997, p. 116.
[3] E. Khan, M. Li, C.P. Huang, Hazardous waste treatment technologies, Water Environ. Res. 79 (2007) 1858–1902.
[4] R.W. Peters, Y. Ku, G.D. Boardman, Wastewater treatment: physical and chemical methods, J. Water Pollut. Control Fed. 6 (1984) 553–568.
[5] T.J. Kanzelmeyer, C.D. Adama, Removal of copper from a metal-complex dye by oxidative pretreatment and ion exchange, Water Environ. Res. 68 (1996) 222–228.
[6] F. Gode, E. Pehlivan, A comparative study of two chelating ion-exchange resins for the removal of chromium(III) from aqueous solution, J. Hazard. Mater. 100 (2003) 231–243.
[7] Z. Aksu, I. Alperişoğlu, Removal of copper ions from aqueous solution by biosorption onto agricultural waste sugar beet pulp, Process Biochem. 40 (2005) 3031–3044.
[8] E. Pehlivan, G. Arslan, Removal of metal ions using lignite in aqueous solution—low cost biosorbents, Fuel Process Technol. 88 (2007) 99–106.
[9] S.A. Khan, R. Rehman, M.A. Khan, Adsorption of chromium(III), chromium(VI) and silver(I) on bentonite, Waste Manage. 15 (1995) 271–282.
[10] M.A. Keane, The removal of copper and nickel from aqueous solution using Y zeolite ion exchangers, Colloids Surf. A 138 (1998) 11–20.
[11] V.K. Gupta, I. Ali, Utilisation of bagasse fly ash (a sugar industry waste) for the removal of copper and zinc from wastewater, Sep. Purif. Technol. 18 (2000) 131–140.
[12] V.K. Gupta, A. Rastogi, Biosorption of lead(II) from aqueous solutions by nonliving algal biomass *Oedogonium* sp. and *Nostoc* sp.—a comparative study, Colloids Surf. B 64 (2008) 170–178.
[13] M.R. Panuccio, F. Crea, A. Sorgonà, G. Cacco, Adsorption of nutrients and cadmium by different minerals: experimental studies and modeling, J. Environ. Manage. 88 (2008) 890–898.
[14] S. Kundu, A.K. Gupta, Analysis and modeling of fixed bed column operations on As(V) removal by adsorption onto iron oxide-coated cement (IOCC), J. Colloid Interf. Sci. 290 (2005) 52–60.
[15] S. Kocaoba, Y. Orhan, T. Akyüz, Kinetics and equilibrium studies of heavy metal ions removal by use of natural zeolite, Desalination 214 (2007) 1–10.
[16] J. Peric, M. Trgo, N.V. Medvidovic, Removal of zinc, copper and lead by natural zeolite—a comparison of adsorption isotherms, Water Res. 38 (2004) 1893–1899.
[17] S. Babel, T.A. Kurniawan, Low-cost adsorbents for heavy metals uptake from contaminated water: a review, J. Hazard. Mater. 97 (2003) 219–243.
[18] M. Rynskyy, B. Buszewski, A.P. Terzyk, J. Namieśnik, Study of the selection mechanism of heavy metal (Pb^{2+}, Cu^{2+}, Ni^{2+} and Cd^{2+}) adsorption on clinoptilolite, J. Colloid Interface Sci. 304 (2006) 21–28.
[19] Y. Al-Degs, M.A.M. Khraisheh, The feasibility of using diatomite and Mn diatomite for remediation of Pb^{2+}, Cu^{2+}, and Cd^{2+} from water, Sep. Sci. Technol. 35 (2000) 2299–2310.
[20] W.H. Kuan, S.L. Lo, M.K. Wang, C.F. Lin, Removal of Se(IV) and Se(VI) from water by aluminum-oxide-coated sand, Water Res. 32 (1998) 915–923.
[21] I.W. Nah, K.Y. Hwang, C. Jeon, H.B. Choi, Removal of Pb ion from water by magnetically modified zeolite, Miner. Eng. 19 (2006) 1452–1455.
[22] M.K. Doula, Removal of Mn^{2+} ions from drinking water by using Clinoptilolite and a Clinoptilolite–Fe oxide system, Water Res. 40 (2006) 3167–3176.
[23] L.C.A. Oliveira, D.I. Petkowicz, A. Smaniotto, S.B.C. Pergher, Magnetic zeolites: a new adsorbent for removal of metallic contaminants from water, Water Res. 38 (2004) 3699–3704.
[24] R.P. Han, W.H. Zou, H.K. Li, Y.H. Li, J. Shi, Copper(II) and lead(II) removal from aqueous solution in fixed–bed columns by manganese oxide coated zeolite, J. Hazard. Mater. 137 (2006) 934–942.
[25] G. Bohart, E.Q. Adams, Some aspects of the behaviour of charcoal with respect to chlorine, J. Am. Chem. Soc. 42 (1920) 523–544.
[26] H.C. Thomas, Heterogeneous ion exchange in a flowing system, J. Am. Chem. Soc. 66 (1944) 1664–1666.
[27] J. Goel, K. Kadirvelu, C. Rajagopal, V.K. Garg, Removal of lead(II) by adsorption using treated granular activated carbon: batch and column studies, J. Hazard. Mater. 125 (2005) 211–220.
[28] R.P. Han, Y.F. Wang, W.H. Yu, W.H. Zou, J. Shi, H.M. Liu, Biosorption of methylene blue from aqueous solution by rice husk in a fixed-bed column, J. Hazard. Mater. 141 (2007) 713–718.
[29] R.P. Han, D.D. Ding, Y.F. Xu, W.H. Zou, Y.F. Wang, Y.F. Li, L.N. Zou, Use of rice husk for the adsorption of Congo red from aqueous solution in column mode, Bioresour. Technol. 98 (2008) 2938–2946.
[30] S.K. Maji, A. Pal, T. Pal, A. Adak, Modeling and fixed bed column adsorption of As(III) on laterite soil, Sep. Purif. Technol. 56 (2007) 284–290.
[31] G.Y. Yang, L. Zhu, Y.H. Li, H.K. Li, R.P. Han, Analysis of FT-IR, XRD and SEM about natural zeolite, Acta Anyang Normal Coll. 2 (2006) 77–78.
[32] W. Mozgawa, The influence of some heavy metals cations on the FTIR spectra of zeolites, J. Mol. Struct. 555 (2000) 299–304.
[33] Z. Aksu, F. Gonen, Biosorption of phenol by immobilised activated sludge in a continuous packed bed: prediction of breakthrough curves, Process Biochem. 39 (2004) 599–613.

[34] V.K.C. Lee, J.F. Porter, G. McKay, Development of fixed-bed absorber correlation models, Ind. Eng. Chem. Res. 39 (2000) 2427–2433.
[35] D. Tiwari, H.U. Kim, S.M. Lee, Removal behavior of sericite for Cu(II) and Pb(II) from aqueous solutions: batch and column studies, Sep. Purif. Technol. 57 (2007) 11–16.
[36] L.N. Zou, Study of adsorption of methylene blue, methyl orange and copper ions from the aqueous solutions by iron-oxide-coated-zeolite, Dissertation of Master Degree, Zhengzhou University, 2008.
[37] R.P. Han, J.H. Zhang, W.H. Zou, H.J. Xiao, J. Shi, H.M. Liu, Biosorption of copper(II) and lead(II) from aqueous solution by chaff in a fixed-bed column, J. Hazard. Mater. 133 (2006) 262–268.